Fast-neutron total and scattering cross sections of ^{182}W, ^{184}W, and ^{186}W

Peter T. Guenther, Alan B. Smith, and James F. Whalen
Applied Physics Division, Argonne National Laboratory, Argonne, Illinois 60439
(Received 25 January 1982)

Neutron total cross sections of ^{182}W, ^{184}W, and ^{186}W were measured from 0.3 to 5.0 MeV at intervals of $\lesssim$50 keV to accuracies of 1 to 3%. Differential elastic- and inelastic-scattering cross sections of the same three isotopes were measured from 1.5 to 4.0 MeV at incident-energy intervals of $\lesssim$200 keV over the angular range 20 to 160 deg. Approximately thirty scattered-neutron groups were observed for each isotope. Prominent among these are excitations attributed to rotational and vibrational bands. The experimental results are interpreted in terms of the statistical and the coupled-channels models with particular attention to the ground-state-rotational and the beta- and gamma-vibrational bands.

[NUCLEAR REACTIONS Measured σ_n (total) of ^{182}W, ^{184}W, ^{186}W, 0.3–5.0 MeV; measured $d\sigma/d\Omega_n$ (elastic and inelastic) 1.5–4.0 MeV, 20–160 deg; statistical and coupled-channels model interpretations.]

I. INTRODUCTION

Fast-neutron interactions with the even isotopes of tungsten are of basic and applied interest. Approximately 85% of the element consists of the isotopes ^{182}W, ^{184}W, and ^{186}W. These isotopes lie in a region of large and changing deformation.[1] They offer an unusual opportunity to study the effects of deformations on the neutron interaction at few MeV energies. Such interactions are a mixture of compound-nucleus (CN) and direct-reaction (DR) processes not easily studied using charged-particle probes. Neutron excitation of collective rotational and/or vibrational levels can be large[2] and anomalous excitation of the ground-state-rotational band (GSRB) in the complimentary region of changing deformation near $A=150$ has been reported.[3] It has been suggested that fast-neutron total cross sections in this region are sensitive to the character of the deformation and observations have been interpreted in terms of quadrupole and hexadecapole deformations.[4,5] Neutron differential-elastic scattering is also sensitive to deformation, particularly at large scattering angles,[6] and direct excitation of the GSRB can be larger than the CN contribution in the several MeV region.[7]

Elemental tungsten finds application in high-temperature nuclear-energy systems. The tungsten isotopes are, in some ways, similar to fission-product and actinide nuclei which are of considerable applied importance but are very difficult to study experimentally. Because of this, applied information is often obtained using theoretical extrapolation, the validity of which is ultimately based upon observations such as those presented here.

The experimental methods employed in this work are outlined in Sec. II. Section III presents the experimental results and Sec. IV deals with their interpretation. More detailed discussion of this work is given in Refs. 6 and 8.

II. EXPERIMENTAL METHODS

The measurements employed three cylindrical metal samples 2 cm in diameter and 2 cm long enriched to $\gtrsim$95 at.% in the primary isotope.[9] The physical and chemical details of the samples are given in Ref. 8.

The neutron total-cross-section measurements were made using the monoenergetic pulsed-beam facility at the Argonne Fast Neutron Generator.[8,10] The ^{7}Li$(p,n)^7$Be reaction was used as a neutron source with the protons incident upon a thin lithium-metal film. The source dimensions were confined to a $\approx$3 mm diameter spot. The proton beam was pulsed at a 2 MHz repetition rate with a pulse duration of $\approx$1 nsec. The mean neutron

energy was determined to within ≈ 10 keV by control of the proton-beam energy and verified by the observation of well-known neutron total-cross-section resonances in a number of materials (e.g., carbon). The neutron source was placed within a 60 cm diameter and 40 cm long cylindrical cavity within a massive shield. That portion of the cavity facing the incident-neutron beam was open. The shield consisted of a tank 2 m in diameter and 2.3 m long filled with a saturated solution of lithium carbonate. A collimator penetrated the shield tank at a zero-degree source-reaction angle. The collimator was constructed of solid copper with a 1 cm in diameter aperture and arranged with the collimator entrance ≈ 20 cm from the neutron source. The collimated neutron beam was incident upon the bases of the cylindrical transmission samples. The latter were located 2 m from the source and mounted upon a wheel with a radius of 20 cm. The wheel provided eight sample positions which contained the three tungsten samples, two voids, and three carbon reference samples. The latter were 2.5 cm in diameter and varied in length from 1 to 4 cm. The wheel was rotated in a stepping motion interchanging samples (or voids) in the neutron beam twenty or more times a minute. No independent monitoring of source intensity was required as the rapid interchange of the samples averaged possible neutron-source fluctuations. A proton-recoil-scintillation detector was placed 4 to 7 m from the samples on the neutron-beam axis. Conventional time-of-flight techniques were used to determine the velocity spectrum of the neutrons passing through the samples and arriving at the detector. The velocity spectra were stored in a digital computer in correlation with the sample (or void) position of the sample wheel. The neutron velocity resolution was sufficient to resolve the primary source-reaction neutron group from the secondary neutron group and from the time uncorrelated background and to define the spectral distribution of the neutron beam to within ≈ 100 keV.

The "observed" neutron total cross sections were calculated from the measured sample transmissions in the conventional manner.[11] Inscattering corrections were estimated, found small, and neglected. Small dead-time corrections were made using a reference-clock pulse introduced into the data-acquisition system. Throughout the tungsten-sample measurements the neutron total cross sections of elemental carbon were concurrently determined with good (better than 2%) agreement with the values reported in the literature.[12]

The neutron-scattering measurements were made using the time-of-flight technique and the Argonne ten-angle scattering apparatus.[7,8] The ^{7}Li$(p,n)^7$Be neutron source was pulsed on for ≈ 1 nsec intervals at a repetition rate of 2 MHz. Incident-neutron energy spreads varied from ≈ 10 to 50 keV. The scattering samples were placed ≈ 13 cm from the source at the focus of the ten flight paths. Generally, the flight paths were ≈ 5.4 m long with some additional measurements made at ≈ 20 m flight paths. Scattering angles were determined to ≤ 1.0 deg. The ten neutron detectors consisted of proton-recoil scintillators. An additional time-of-flight detector monitored the primary-source intensity. The relative energy-dependent responses of the detectors were determined by the observation of neutrons emitted at the spontaneous fission of ^{252}Cf and/or by the observation of monoenergetic neutrons scattered from hydrogen over a range of scattering angles.[13] The absolute normalizations of the relative responses were determined by scattering neutrons from hydrogen (CH_2) at each measurement energy. These calibration procedures implied that the tungsten scattering cross sections were determined relative to the well-known H(n,n) cross sections.[14] Off-line analysis reduced the observed velocity spectra to cross sections as described in Ref. 6. All scattering-cross-section results, including those associated with the H(n,n) reference standard, were corrected for angular-resolution, beam-attenuation, and multiple-event effects using Monte Carlo and analytical procedures.[6] The multiple-scattering corrections employed an explicit Monte Carlo simulation of the experimental measurements giving consideration to elastic scattering, up to 20 inelastically-scattered neutron groups, and to inelastic-neutron evaporation spectra where relevant. The initial input to the calculations was taken from the measured neutron total and scattering cross-section results. Generally, neutrons were followed through either three or five collisions within the sample and those emitted from the sample were sorted into 24 equally-spaced angular bins. The angular-bin selection was a compromise between statistical uncertainty and angular resolution at the extreme minima of the elastic-scattering angular distributions. In such regions both the measurements and the simulations were subject to larger statistical uncertainties. The Monte Carlo simulation was verified by studies of neutron scattering from bismuth samples varying in mass by factors of 8. Throughout the scattering measurements frequent determinations of the well-known C(n,n) cross sections[12] were made in order to verify the performance of the measurement system.

III. EXPERIMENTAL RESULTS

A. Neutron total cross sections

Measurements were made in three periods with energy resolutions of ≈ 20 to 50 keV and to statistical accuracies of 1% to 3%. The results were generally consistent to within the statistical uncertainties. The observed cross sections were explicitly relevant to the specific sample thicknesses employed in the measurements. Poenitz *et al.*[15] have shown that self-shielding corrections can significantly distort broad-resolution heavy-element total cross sections well into the 100 keV region with observed values that can be significantly smaller than the "true" or infinitely-thin-sample results. The self-shielding correction can be calculated from the statistical properties of the underlying fluctuating structure or determined experimentally using a wide range of transmission-sample thicknesses. The latter approach was not explicitly possible in the present case as the integrity of rare samples could not be destroyed. Therefore the calculational approach was chosen. The potential cross sections and average resonance properties were derived from optical-model phase shifts using an optical potential that described the low-energy behavior of the energy-averaged total cross sections. Assuming a single-level Breit-Wigner formulation, average level spacings from a Fermi gas model, and Wigner and Porter-Thomas distributions of level spacings and width fluctuations, respectively; a Monte Carlo simulation of the resonance cross sections was constructed from which the correction factors for the present experiments were inferred. Details of this calculational procedure are given in Ref. 15. The effect of these correction factors was large at low energies (nearly 20% at 100 keV) and decreased with increasing energy to a negligible amount at 1.0 MeV.

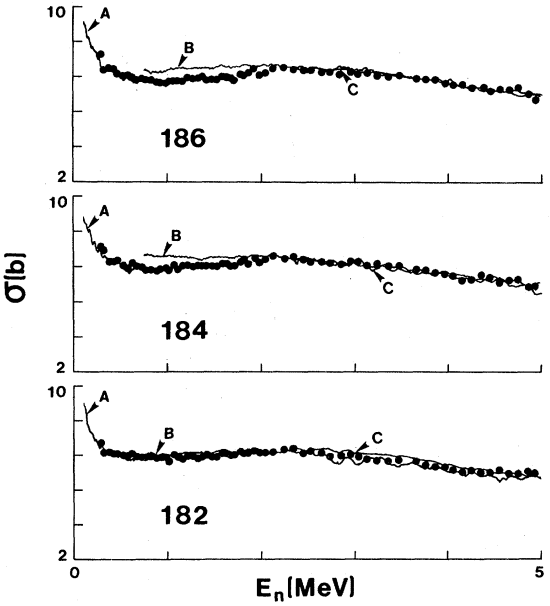

FIG. 1. Neutron total cross sections of ^{182}W, ^{184}W, and ^{186}W. The present experimental results are indicated by data points. Curves denote averages of previously reported experimental results referenced as follows: $A = 10$ keV average of Ref. 17, $B = 100$ keV average of Ref. 18, and $C = 100$ keV average of Ref. 19.

It was possible to experimentally test the above correction factors for elemental tungsten. Assuming an "element" consisting of even isotopes (85% abundant), elemental correction factors were derived from the above isotopic factors. These elemental correction factors were applied to observed elemental total cross sections determined with a wide range of sample thicknesses at several incident energies. The resulting corrected elemental cross sections were constant with sample thickness to within the $\lesssim 1\%$ statistical accuracies of the measurements.[16] This elemental test gave confidence to the above isotopic corrections. Low-energy isotopic total cross sections previously reported from this laboratory[17] used the same samples as the present work. Therefore similar corrections were applied to the previously determined low-energy values.

The present results, measured at various times, were combined and averaged over 50 keV intervals to 2.0 MeV and over 100 keV intervals at higher energies. The statistical uncertainties of the averaged values were generally $\lesssim 1\%$. Systematic uncertainties were small except at low energies where the self-shielding factors introduced an additional several percent uncertainty. These averaged results are illustrated in Fig. 1. Qualitatively, the results for the three isotopes are similar. Quantitatively, there are magnitude and energy-dependent-shape differences beyond the experimental uncertainties.

There apparently are only three sets of previously reported data that are directly comparable with the present total-cross-section results. Whalen[17] has reported results for all three isotopes from 0.1 to 0.65 MeV. As corrected for self-shielding, they are in good agreement with the present values as illustrated in Fig. 1. Martin *et al.*[18] have reported total cross sections for these isotopes from ≈ 0.7 to 15.0 MeV. The ^{184}W and ^{186}W results of Ref. 18 are qualitatively inconsistent with the present values as

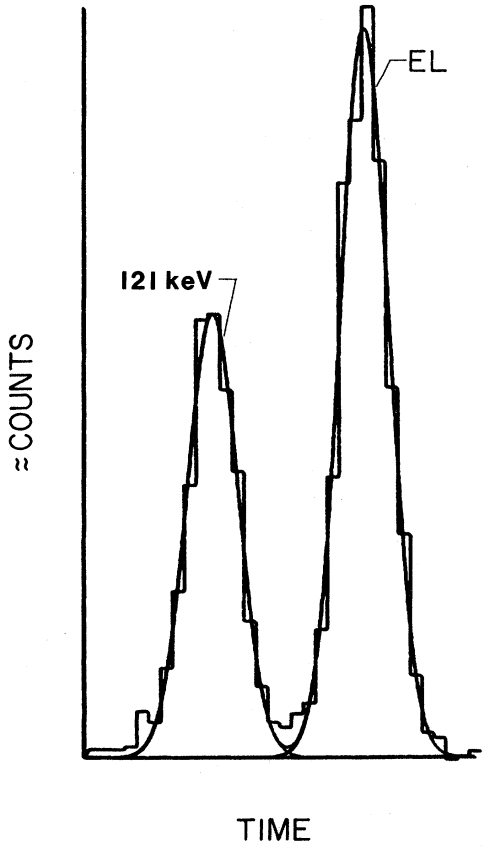

FIG. 2. Neutron time-of-flight spectrum obtained by scattering 1.8 MeV neutrons from ^{186}W at an angle of 115 deg (histogram). The flight path was 5.5 m. The smooth curve indicates the result of fitting two Gaussian distributions to the measured values corresponding to the elastic- and inelastic- (observed $E_x = 121$ keV) neutron groups. The time scale is ≈ 0.75 nsec/channel.

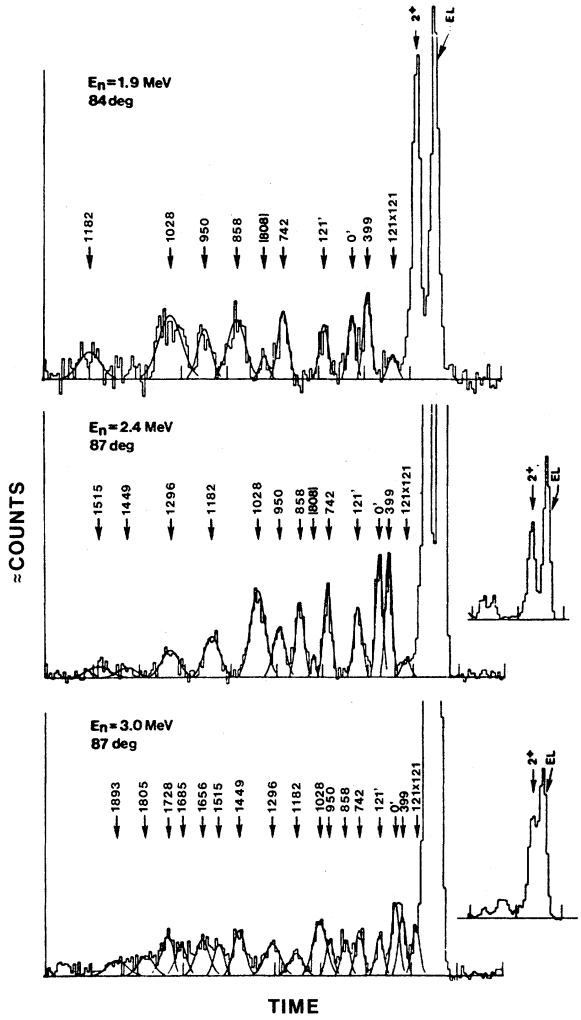

FIG. 3. Time-of-flight spectra obtained by scattering neutrons from ^{186}W using instrument settings selected for the observation of higher-energy excitations. The flight path was ≈ 5 m and the time/channel ≈ 1.5 nsec. Incident energies and scattering angles are numerically given in the respective sections of the figure. Level energies (in keV) are numerically indicated. Primed quantities refer to events due to the second group from the source reaction. Plural scattering is also indicated. The inelastic groups are emphasized with Gaussian "eye-guides."

shown in Fig. 1. The discrepancies are not simply attributable to sample-density effects or the above self-shielding phenomena. Foster and Glasgow[19] have reported results for these isotopes over the energy range 2.5 to 15.0 MeV. Their values are generally consistent with those of the present work (see Fig. 1). The isotopes employed in the present study make up $\approx 85\%$ of the element. Thus, assuming the total cross sections of the remaining 15% of the isotopes are similar, the weighted average of the present results should agree with the elemental values. An inspection of reported elemental information[20] indicates that this is true.

B. Elastic neutron scattering

The primary problem in the elastic-scattering measurements was the resolution of the elastic-neutron group from the inelastic components corresponding to the excitation of the ≈ 110 keV level. Most of the measurements were made with flight paths of ≈ 5.4 m. At higher energies some measurements were made with ≈ 20 m flight paths in order to improve the resolution of the elastic-scattered components and the results were also used to correct the shorter-flight-path values, measured at similar energies, for unresolved inelastic-neutron contributions. A wide variation of instrument

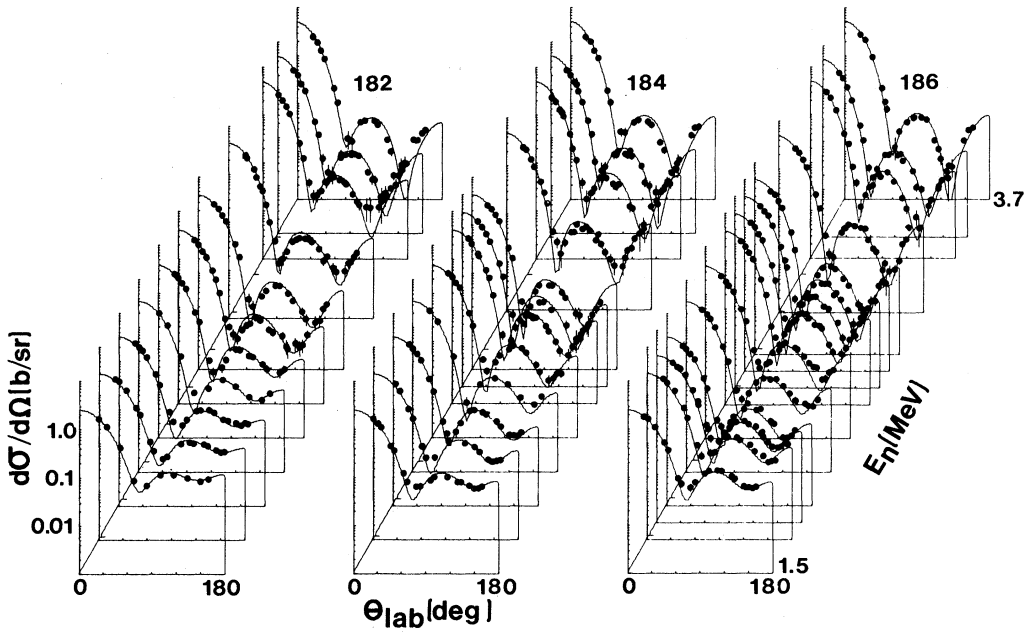

FIG. 4. Differential-elastic-scattering cross sections of ^{182}W, ^{184}W, and ^{186}W. The present experimental values are noted by data symbols and curves indicate the results of calculation as described in the text.

parameters was employed in the measurements, selected to emphasize particular aspects of the observations. Therefore, there is no "representative" time-of-flight spectrum. A number of illustrative velocity spectra are given in Ref. 8. Two of these examples, directed toward very different measurement objectives, are shown in Figs. 2 and 3. They should not be construed as representative of results obtained in all aspects of the measurements.

Measurements were made at intervals of $\lesssim$200 keV from 1.5 to 4.0 MeV and generally at $\gtrsim$20 scattering angles distributed between 20 and 160 deg. At some energies a large number of differential cross-section values were obtained (e.g., $\approx$100 at 3.0 MeV) and in these instances the data were averaged to reduce the angular distributions to between 20 to 30 differential values. The results of the measurements are summarized in Fig. 4. The quality of the angular distributions varies depending on the particular experimental conditions. Generally the statistical accuracies were several percent and frequently $\lesssim$1%. The detector normalizations were reproducible to within $\approx$4%. Correction procedures (e.g., for multiple events) introduced a 1% to 5% uncertainty except near the extreme minima of the distributions where the correction uncertainties could be larger. The H(n,n) reference cross sections were believed known to 1%. In addition, uncertainties were influenced by the experimental resolution. In some cases the resolution was very good and was not a factor in estimating uncertainties. In other instances the resolution was not as satisfactory and consequently the respective cross-section uncertainties were larger. The total uncertainties, reflecting the above factors, are given by the error bars of Fig. 4.

The measured differential-elastic-scattering distributions were least-square fitted with eight-order Legendre-polynomial series. The fitting procedures were constrained to be consistent with "Wick's limit"[21] and to provide a reasonably smooth energy dependence of the extrapolated 180 deg values. Some results of these fitting procedures are shown in Fig. 5 and more are given in Ref. 8. The fitting also provided the angle-integrated elastic-scattering cross sections shown in Fig. 6. The latter are believed known to between 5% and 7% and the results are generally consistent to well within these uncertainties.

Comparable previously reported elastic-scattering results appear limited to the low-energy work of Lister *et al.*[22] and the 3.4 MeV results of Delaroche *et al.*[23] The present results reasonably extrapolate to the lower-energy values of Ref. 22, as illustrated in Fig. 6, and are similar to the differential-cross-section values of Ref. 23 as shown in Fig. 5.

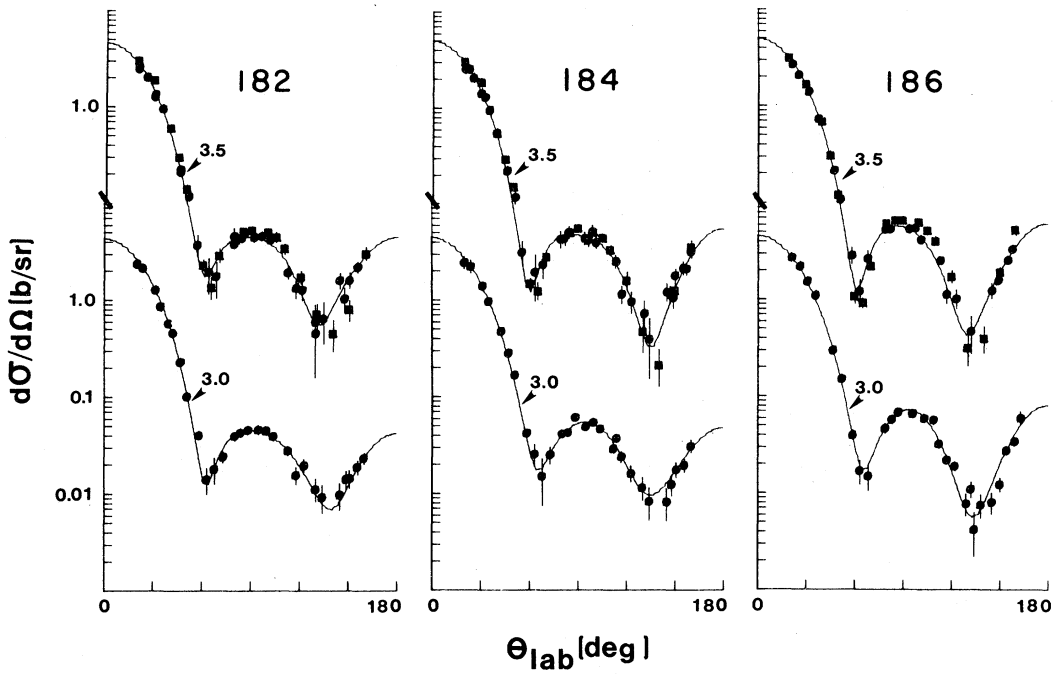

FIG. 5. Illustrative differential-elastic-scattering cross scattering sections of ^{182}W, ^{184}W, and ^{186}W. The present measured values are indicated by circular symbols (with numerical energy values), those of Ref. 23 by squares (measured at 3.4 MeV). Curves note results of fitting a Legendre-polynomial series to the present experimental values.

C. Neutron inelastic scattering

The experimental definition of a given inelastic-neutron group was sensitive to the particular instrument configuration and was optimum over a limited energy range. Therefore measurements were made in systematic incident-energy steps so that the inelastic identification in regions of optimum definition could be followed into regions of marginal resolution. Where at all practicable, artifacts due to multiple events and the second neutron group from the source reaction were identified and removed. An example is given in Fig. 3.

The observed inelastic-neutron excitation energies were calculated from the measured incident energies, flight paths, and flight times. A neutron group was accepted for the determination of excitation energy when reliably observed on at least five occasions each involving several detectors. The observed excitation energies were defined as the simple averages of the respective measured values with the uncertainties expressed as the root mean square (rms) deviations from the means. Approximately 30 excitations were so identified in each of the three isotopes, as summarized in Table I. Many of these corresponded to energies of $\gtrsim 1.5$ MeV where the experimental resolution was not comparable with the expected detail of the structure. Even at excitation energies of 1.5 MeV many of the observed neutron groups were composites of several components. Plots of the observed level density versus excitation energy qualitatively behaved in the expected exponential manner between 1.5 and 2.0 MeV and then departed from the exponential form as would be expected from incomplete experimental resolution. Thus the majority of the values of Table I should be considered observables in the context of the experimental resolutions. However, the results of Table I are reasonably consistent with previously reported structure information as illustrated in Fig. 7.

The inelastic-scattering cross sections were derived from the observed velocity spectra in a manner analogous to that employed for elastic scattering. The most accurate cross sections were sought rather than the best possible resolution of the components. The angle-integrated cross sections were determined by least-square fitting the differential values with Legendre-polynomial series constrained to provide a smooth energy dependence of the extrapolated 0 and 180 deg cross sections.

At excitations of $\lesssim 0.8$ MeV the inelastic scatter-

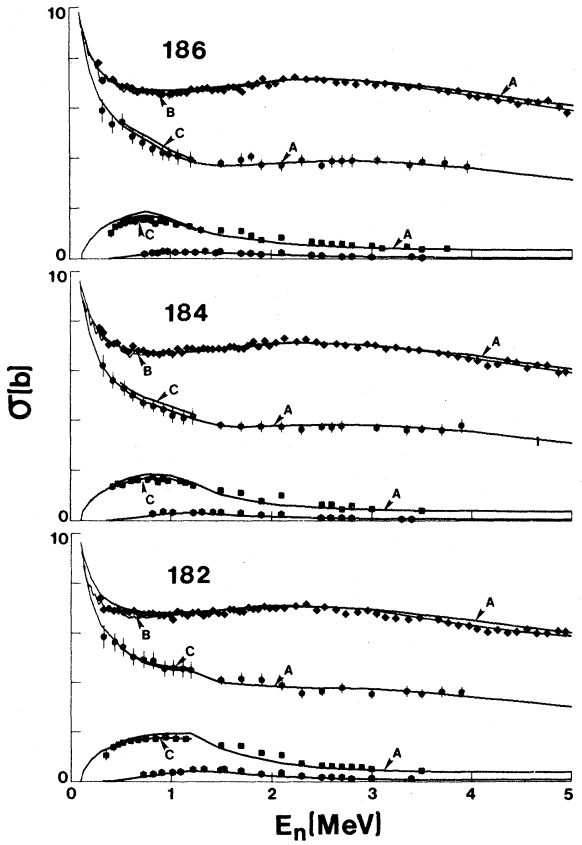

FIG. 6. Measured and calculated cross sections of ^{182}W, ^{184}W, and ^{186}W. The present experimental values (and those of Ref. 22) are indicated by data symbols as: ◆ = total cross section, ● = elastic scattering, ■ = inelastic scattering to the first 2+ level, and ⧫ = inelastic scattering to the first 4+ level. Curve "*B*" is an eye-guide constructed through the present measured total cross sections and those of Ref. 17. Curves "*A*" (or unmarked) result from calculations using the base model of the text and curves "*C*" result from modified CN calculations as described in text.

ing was dominated by contributions from the GSRB. Scattered-neutron anisotropy associated with the first two GSRB levels (2+ and 4+) rapidly increased with energy as shown in Figs. 8 and 9. The corresponding angle-integrated cross section values are shown in Fig. 6. Qualitatively, the cross sections of these isotopes are similar but there are detailed differences in both shape and magnitude.

Above excitation energies of ≈0.8 MeV the scattered-neutron angular distributions were essentially isotropic but small anisotropies were observed for excitations corresponding to 0+ levels and to beta- and gamma-vibrational bands as discussed below. Some of the resulting angle-integrated inelastic-scattering cross sections are illustrated in Fig. 10 and more comprehensive illustrations, corresponding to the levels of Table I, are given in Ref. 8.

Uncertainties associated with the above differential and angle-integrated cross sections varied from 5% in the best cases to as much as 30% to 50% in marginally observed cases. The origin of these uncertainties was similar to that outlined above in the context of elastic scattering with greater emphasis on subjective judgment. The uncertainty estimates are supported by the reproducibility of results obtained over an extended period of time. In addition, the sum of elastic- and inelastic-scattering components is generally consistent with the observed total cross section as discussed in Ref. 8.

Apparently only two previous measurements of inelastic-scattering cross sections comparable with the present results have been reported. The lower-energy results of Lister *et al.*[22] reasonably extrapolate to those of the present work as illustrated in Fig. 6. Delaroche *et al.*[23] have reported cross sections for the excitation of the GSRB at an incident energy of 3.4 MeV. The latter are generally consistent with the results of the present work as illustrated in Ref. 8.

IV. PHYSICAL INTERPRETATION AND COMMENT

The interpretation was based upon the coupled-channels model.[24] Neutron cross sections were calculated using the computational code JUSTSO, augmented by the spherical optical-model code ABAREX.[25] JUSTSO determines transmission coefficients from the deformed potential and calculates the compound nucleus (CN) contributions using the Hauser-Feshbach formula[26] with the width-fluctuation and correlation corrections. The latter corrections were based upon the formalism of Moldauer[27] which considers the enhancement of elastic- and inelastic-neutron processes in the coupled channels. The calculations explicitly considered the inelastic excitation of levels to ≈1.5 MeV using the energies, spins, and parities of Ref. 1. CN competition due to higher-energy levels was approximated using the statistical level parameters of Gilbert and Cameron.[28]

The potential of Delaroche *et al.*,[23] defined in Table II, was used as the "base" model with coupling of the first three levels of the GSRB (0+, 2+, and 4+). That potential was generally suitable for the present interpretations and was supported by extensive parameter studies by one of the authors (P.T.G.) reported elsewhere.[6,8] The calculated results were compared with the present experimen-

TABLE I. Observed excitation energies.

Number	E_x (keV)	Number	E_x (keV)
	Energies for ^{182}W[a]		
1	102 ±8	19	2059 ±25
2	326 ±15	20	2121
3	671 ±14	21	2185
4	1138 ±16	22	2247
5	1229 ±12	23	2299
6	1281 ±22	24	2382 ±28
7	1309 ±18	25	2468 ±15
8	1357 ±21	26	2543 ±22
9	1428 ±38	27	2615 ±15
10	1492 ±15	28	2690
11	1539 ±16	29	2768
12	1618 ±24	30	(2819)
13	(1678)	31	(2867)
14	1745 ±23	32	(2932)
15	1792 ±20	33	(2979)
16	1858 ±20	34	(3022)
17	1914 ±20	35	(3062)
18	1988 ±21		
	Energies for ^{184}W		
1	111 ±10	16	1911 ±25
2	365 ±20	17	2008 ±30
3	737 ±32	18	2105 ±37
4	905 ±24	19	2155 ±34
5	1000 ±24	20	2240 ±25
6	1125 ±17	21	2324 ±24
7	1237 ±31	22	2440
8	1323 ±43	23	2520
9	1376 ±23	24	2580
10	1435 ±17	25	2638
11	1528 ±12	26	2663
12	1613 ±18	27	2735
13	1667 ±13	28	(2811)
14	1725 ±29	29	(2866)
15	1787 ±32	30	(2918)
	Energies for ^{186}W		
1	121 ±7	19	2004 ±15
2	399 ±10	20	2073 ±12
3	742 ±7	21	2118 ±12
4	858 ±18	22	2177 ±13
5	950 ±21	23	2241 ±26
6	1028 ±32	24	2347 ±18
7	1182 ±26	25	2406 ±12
8	1296 ±31	26	2462
9	(1397 ±35)	27	2552
10	1449 ±24	28	2643
11	1515 ±35	29	(2713)
12	1589 ±19	30	(2768)
13	1656 ±21	31	(2820)
14	(1685 ±10)	32	(2868)
15	1728 ±25	33	(2933)
16	1805 ±15	34	(2979)
17	1893 ±29	35	(3023)
18	1942 ±35	36	(3063)

[a]Uncertainties are rms deviations from the simple mean determined from at least five measurements. No uncertainty is given if less than five observations were available. Parentheses indicate tentative assignments of observed quantities often due to the excitation of several levels.

tal values and with lower-energy results[17,22] previously reported from this laboratory. The neutron total cross sections received first attention as they were accurately measured and unambiguously calculable. Next, angle-integrated cross sections associated with the GSRB were considered. These were reasonably well defined by the measurements and easily calculable at low energies where the CN process dominates and at high energies where the cross sections are largely due to DR processes. Differential cross sections associated with the GSRB were given less attention as they were often small and consequently the associated uncertainties were relatively large. Cross sections for the excitation of levels above the GSRB were calculated using the coupled-channels model to excitations of ≈ 1.2 MeV and with an equivalent spherical model at higher energies. No attention was given to low-energy strength functions as they were experimentally uncertain and there remain questions as to their interpretation.[29]

The measured neutron total cross sections are compared with those calculated from the base model in Fig. 6. For ^{184}W and ^{186}W the agreement is good but for ^{182}W the calculated values are significantly larger than the measured results below ≈ 1.0 MeV. The latter were sensitive to the above self-shielding corrections but above ≈ 0.4 MeV this effect was very small. Measured and calculated angle-integrated cross sections associated with the GSRB are also compared in Fig. 6. The base model gives a good account of the observed elastic-scattering cross sections. The calculated excitations of the GSRB $2+$ ($E_x \approx 0.11$ MeV) levels are slightly larger than the observed values at $\lesssim 1.0$ MeV; at high energies (e.g., $\gtrsim 3.0$ MeV), where the DR processes dominate, the agreement is reasonably good. In the intermediate-energy region there are differences between measured and calculated results that decrease with increasing target mass. Measured and calculated cross sections for the excitation of the GSRB $4+$ ($E_x \approx 0.37$ MeV) levels are in reasonable agreement over the range of appreciable cross-section magnitudes (see Fig. 6). There is no anomalous behavior of the $4+$ level excitations as, for example, reported for the samarium isotopes.[3] The calculated excitations of the GSRB $6+$ levels (e.g., the 671 keV level in ^{182}W, shown in Fig. 11) are notably smaller than the measured values by amounts not reasonably attributable to direct excitations. These differences may well be of an experimental origin as the respective cross sections are very small and difficult to measure with reliability.

The measured differential-elastic-scattering cross

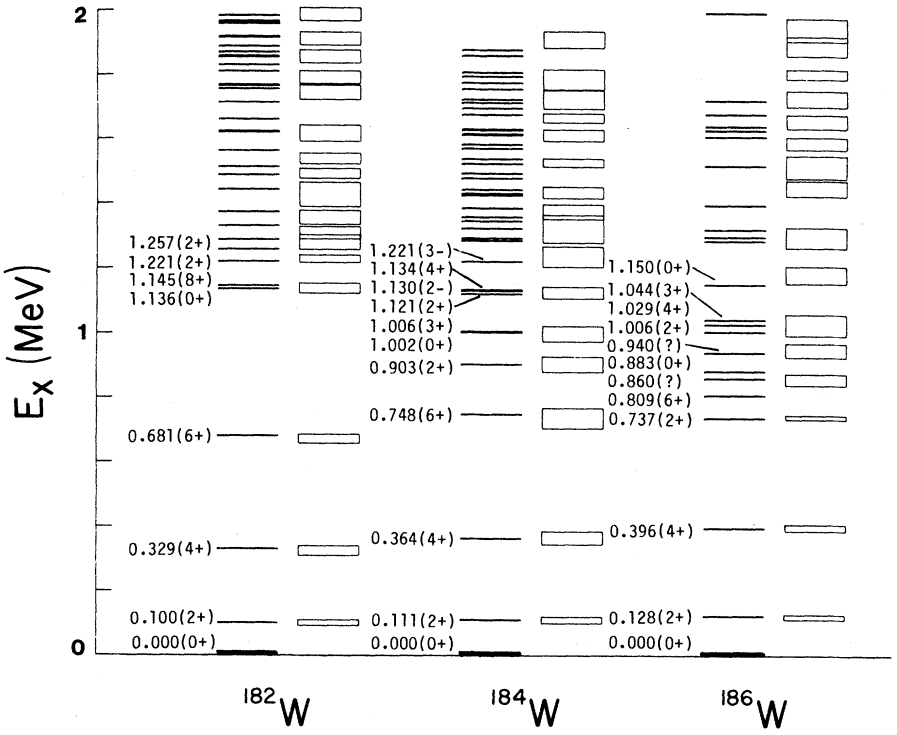

FIG. 7. Excitations observed in the present neutron-scattering experiments (boxes) compared with the level structure given in the compilation of Ref. 1. Excitation energies (MeV) and J^{π} values are given to excitations of ≈ 1.2 MeV. More details of the structure information are given in Ref. 1.

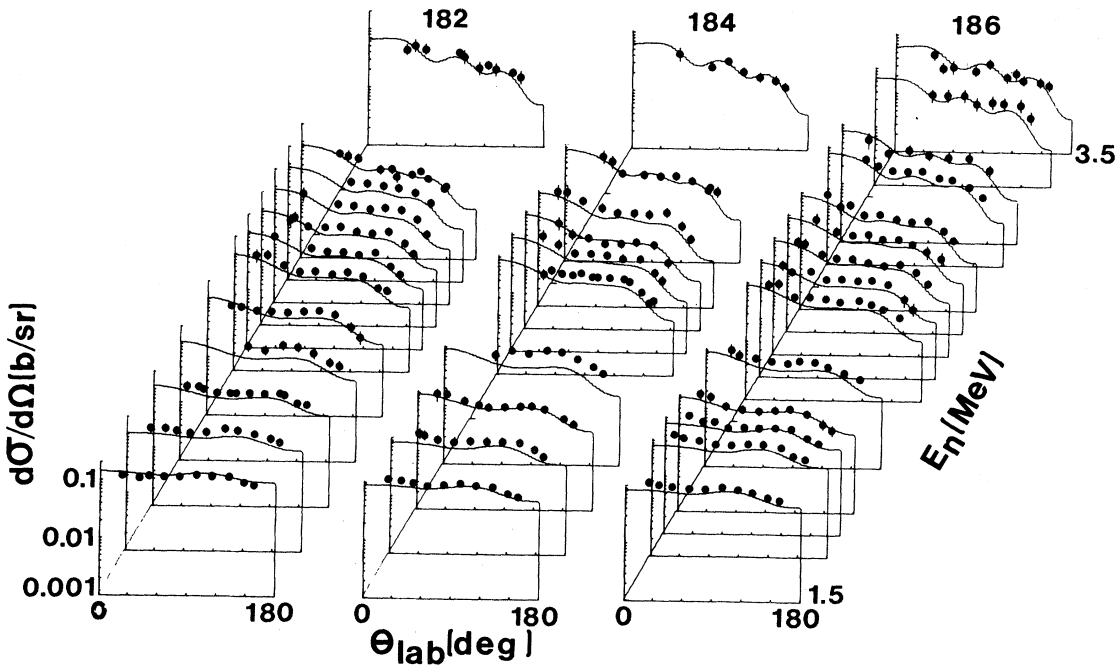

FIG. 8. Comparison of measured and calculated neutron-differential-scattering cross sections for the excitation of the first 2 + states of ^{182}W, ^{184}W, and ^{186}W. The experimental results are indicated by data symbols and those obtained via calculation by curves.

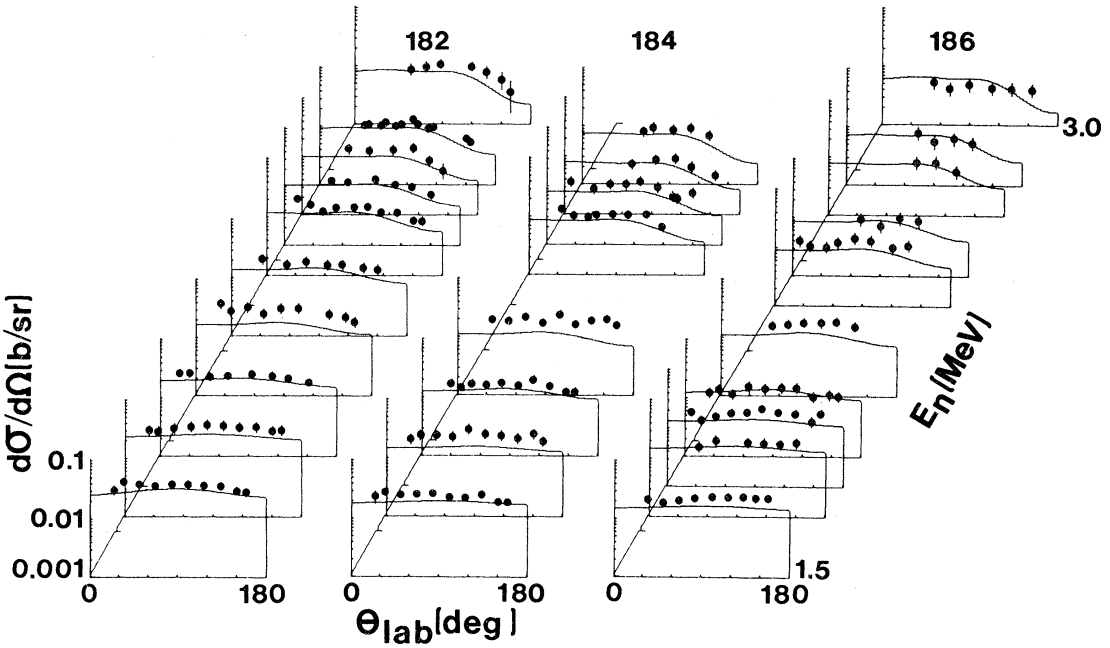

FIG. 9. Comparison of measured and calculated neutron-differential-scattering cross sections for the excitation of the first 4+ states of ^{182}W, ^{184}W, and ^{186}W. The experimental results are indicated by data symbols and those obtained via calculation by curves.

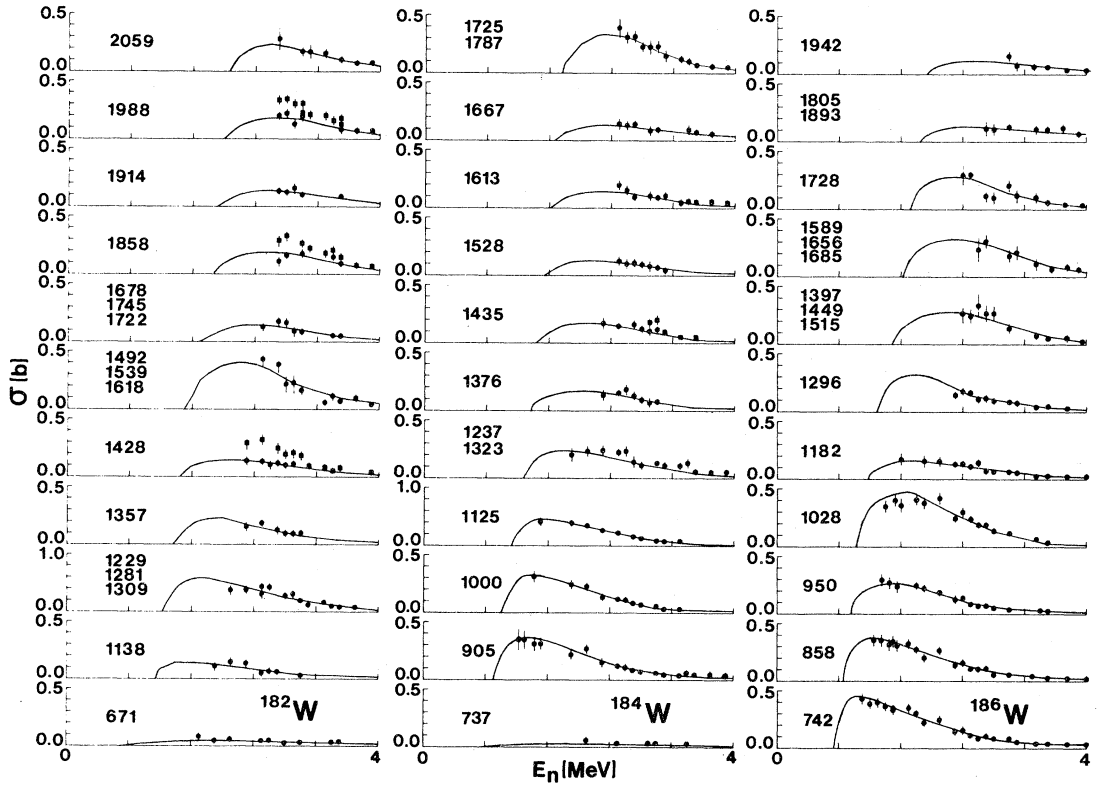

FIG. 10. Illustrative inelastic-excitation cross sections of ^{182}W, ^{184}W, and ^{186}W. Circular data points indicate the present experimental results, squares where the noted values are summed with the previous and lower-energy excitation. Curves are "eyeguides." Observed excitation energies are numerically shown in keV.

TABLE II. Base tungsten potential parameters taken from Ref. 23, where all radii are defined as $R=R_0A^{1/3}$, the real potential has the Saxon form, the imaginary potential is the surface-derivative of the Saxon form, the spin-orbit strength is taken to be 6.0 MeV and of the Thomas form, quadrupole deformations are 0.223 (182), 0.209 (184), and 0.203 (186), and hexadecapole deformations are −0.054 (182), −0.056 (184), and −0.057 (186).

Real potential		
$V=49.90-16\left[\frac{N-Z}{A}\right]-0.25E$		MeV
$R_0=1.26$		F
$A=0.63$		F
Imaginary potential		
$W=4.93-8\left[\frac{N-Z}{A}\right]+1.3E^{1/2}$		MeV
$R_0=1.28$		F
$A=0.47$		F

sections are compared with those calculated from the base model in Fig. 4. The agreement is generally good but there are differences, notably near the minima of the distributions where the experimental values may be somewhat distorted by approximations used in the multiple-event corrections.[16] Comparisons of measured and calculated differential cross sections for the excitations of the GSRB 2+ and 4+ levels are shown in Figs. 8 and 9. The shapes of measured and calculated results are reasonably consistent though there are magnitude differences, particularly in the mid-energy range, as noted above.

The results of calculations of the inelastic-excitation cross sections of levels from the GSRB to excitations of ≈1.5 MeV are shown in Fig. 11. Higher-energy excitations were not explicitly calculated as the requisite level information remains fragmentary. The agreement with the experimental values is best for ^{186}W but there is a general tendency for the calculated results to be smaller than the measured values. This was particularly so for ^{182}W where the calculations are most sensitive to the statistical level properties governing channel competition. These differences suggest that the level densities implied by the parameters of Ref. 28 are too large in this mass-energy region. The agreement between calculation and experiment could have been improved by the adjustment of the statistical level parameters but that is a pragmatic procedure that was not pursued.

Level ambiguities hampered the above calculations as illustrated by the 1182 ± 26 keV level in ^{186}W. This level was observed a number of times with reasonable reliability. The reported 1150 keV level[1] is at a nearby energy but cross sections calculated assuming its reported 0+ character were a factor of 2 smaller than the measured values (see Fig. 11). Inclusion of the expected 4− member of the octupole-vibrational band did not appreciably improve the situation. However, the assumption of a 2+ level led to results consistent with observation. Recent interacting-boson-model calculations suggest a 2+ level at 1156 keV with small $B(E2)$ coefficients for γ-ray transitions to the 0+ and

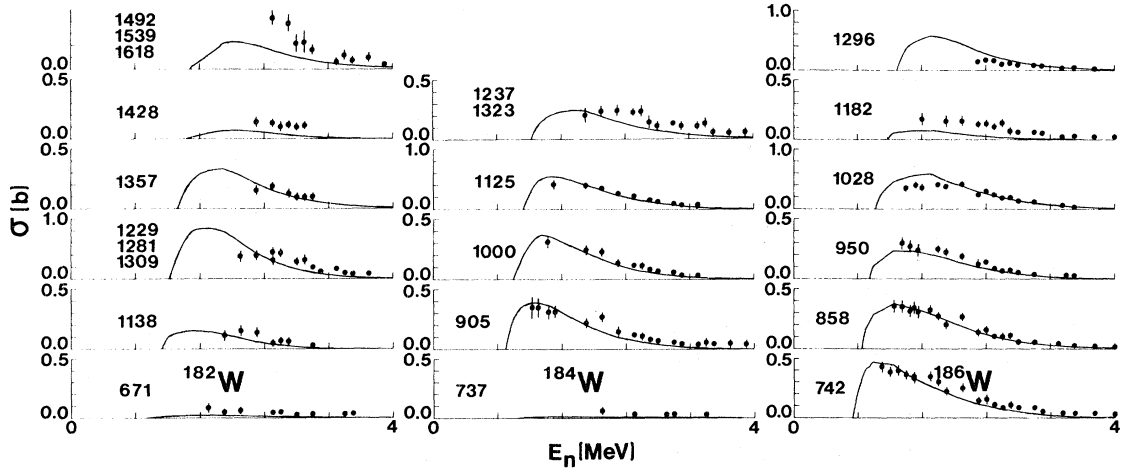

FIG. 11. Comparison of measured and calculated inelastic excitation cross sections of ^{182}W, ^{184}W, and ^{186}W. The data points represent the present measured values corresponding to the observed excitation energies noted in keV on the sections of the figure. Curves indicate the results of calculations as described in the text. The requisite J^π values were explicitly taken from Ref. 1.

2+ members of the GSRB.[30] Results of preliminary $(n;n',\gamma)$ measurements by one of the authors (P.T.G.) show strong γ-ray transitions from a 1153 $\pm$ 2 keV level to the 2+ member of the GSRB with no companion transitions to the 0+ ground state. These observations favor the reported 0+ assignment. No other γ-ray transitions consistent with a 2+ level at $\approx$1180 keV were observed. Thus, in this example, a dichotomy remains and it is representative of other level uncertainties.

The discrepancy between measured and calculated low-energy total cross sections of ^{182}W (cited above) was troubling and causes were sought. Prominent among these were quadrupole and hexadecapole deformations. Elastic-scattering distributions were sensitive to β_4 and appreciable variations in this parameter were not attractive.[6] However, if β_2 was reduced from the 0.223 of Table II to $\approx$0.205 (e.g., to a value approximately equivalent to that of the other isotopes) the description of the measured low-energy total cross sections of ^{182}W was improved and, concurrently, there was a modest improvement in the descriptions of the excitation of the GSRB 2+ level and of the large-angle elastic-scattering cross sections.[6,8] The smaller β_2 was not consistent with other experimental evidence[1] or with the assumption that these isotopes lie in a transitional region from deformation to sphericity. Perhaps a smaller β_2 reflects some other aspect of collective deformation, such as variations in coupling schemes or higher-order deformation, not addressed in the present calculations.

The above CN calculations employed the correction factors of Moldauer[27] which assume a channel degree of freedom (ν) of $\approx$1.8 resulting in elastic-enhancement factors of $\approx$2.1. The correction factors are sensitive to resonance pole-residue amplitudes and to pole spacings. Alternate choices of ν can effect the calculated results. The calculations were repeated assuming $\nu=1.0$ with results illustrated by the "C" curves of Fig. 6. The calculated elastic scattering remained reasonably consistent with observation. The calculated excitation of the GSRB 2+ level was reduced, relative to that obtained with $\nu=1.8$, by 5 to 10% with results in better agreement with experiment. The effect of other choices of ν are discussed in Ref. 6. These comparisons indicate that the ability to quantitatively calculate CN cross sections is considerably predicated upon the pragmatic adjustment of correction factors to achieve agreement with observed values.

The direct excitation of levels beyond the GSRB was examined assuming the model parameters of Table II, the separability of DR and CN processes, and the above GSRB coupling scheme. These assumptions were reasonable for qualitative investigation but it is emphasized that coupling schemes do influence the selection of model parameters. The most promising isotope for examination was ^{186}W where the γ-vibrational-band (GVB) head is at low energies (i.e., the 2+ level at 738 keV,[1] observed at 742 keV). The above CN calculations generally underestimate the excitation of this level (see Fig. 11). This suggests the presence of an additional DR component and this is supported by the neutron angular distributions observed at higher energies (see Fig. 12) which are asymmetric about 90 deg, in contrast with those associated with neighboring levels.[6,8] The latter are the octupole-vibrational-band head at 950 keV and the observed composite level at

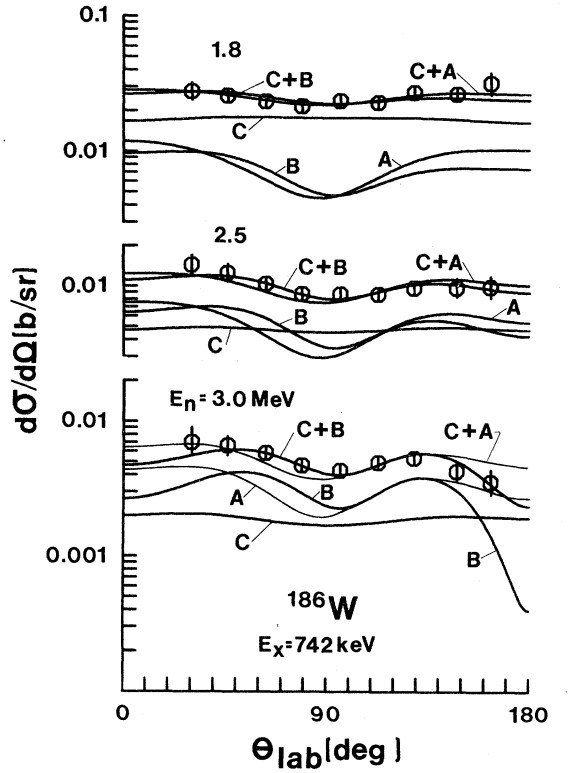

FIG. 12. Angular distributions of neutrons scattered after the excitation of the γ-vibrational-band head at 742 keV in ^{186}W. Incident neutron energies are 1.8, 2.5, and 3.0 MeV. Present experimental values are indicated by circular symbols. Curves denote: $C=$ CN component, $A=$ DR component from coupling scheme (A) of the text, $B=$ DR component from scheme (B) of the text, and $C+A$ and $C+B=$ the respective sums of DR and CN contributions.

858 keV consisting of the second member of the GVB (3 +) and the β-vibrational-band (BVB) head (0 +). Two alternate coupling schemes were assumed; coupling scheme (A) GSRB (0 + , 2 + , 4 +) and GVB (2 + , 3 +), and coupling scheme (B) GSRB (0 + , 2 + , 4 +), GVB (2 + , 3 +), and BVB (0 +). The spins and parities of the respective coupled levels are parenthetically indicated. The coupling-strength parameter,[31] η_{GVB}, was treated as an empirical parameter and η_{GVB} [in scheme (B)] was assumed equal to 0.1. η_{GVB} was determined by least-squares adjusting the amplitudes of the DR and CN contributions to the observed (738 keV) angular distributions at a number of energies between 1.8 and 3.0 MeV in order to optimize the agreement with the experimental results. The DR component magnitude was largely determined by η_{GVB} and thus the fitting procedure implied η_{GVB} values. CN magnitudes were essentially governed by channel competition, the shape remaining approximately constant. Thus the fitting procedures minimize channel-competition uncertainties mainly attributable to uncertainties in statistical level parameters. Coupling scheme (B) resulted in $\eta_{GVB}=0.15$, essentially constant ($\approx\pm 10\%$) with energy. The η_{GVB} obtained with coupling scheme (A) was strongly energy dependent, decreasing from ≈ 0.13 at 1.8 MeV to ≈ 0.07 at 3.0 MeV. The resulting η_{GVB} was employed to calculate the composite DR and CN cross sections at a number of energies using JUSTSO with the adjusted CN contributions. Illustrative comparisons of the calculated and experimental values are shown in Fig. 12. At 1.8 MeV the results obtained with the two coupling schemes are similar to each other and to the experimental results. At 2.5 MeV coupling scheme (B) gives a somewhat better description of the experimental results. At 3.0 MeV the results obtained with coupling scheme (B) remain consistent with experiment while those obtained with coupling scheme (A) diverge from the data. These comparisons and the constancy of η_{GVB} with energy support the validity of coupling scheme (B). Moreover, scheme (B) results in a somewhat better description of the neutron angular distributions associated with the 858 keV level which are partly due to the second (3 +) member of the GVB. The above suggests that coupling schemes should be extended beyond the GSRB, in particular including both β- and γ-vibrational bands. Doing so will influence the choice of underlying model parameters. However, rigorous treatments of such complex coupling schemes require experimental accuracies beyond those thus far achieved.

V. SUMMARY REMARKS

Results of the present experiments, together with those previously reported from this laboratory,[17] define the neutron total cross sections of ^{182}W, ^{184}W, and ^{186}W from 0.1 to 5.0 MeV. These results resolve previous experimental discrepancies and highlight the importance of resonance self-shielding effects at low energies.

The present measurements, and those of Ref. 22, provide a quantitative determination of the neutron differential-scattering cross sections of these three isotopes from ≈ 0.3 to 4.0 MeV. Approximately 30 scattered-neutron components were observed for each isotope. Prominent among these were those associated with the GSRB. The observed scattered-neutron groups were qualitatively consistent with reported level structure[1] but quantitative level uncertainties persist, particularly for ^{186}W.

Results of coupled-channels calculations employing the model and coupling scheme of Delaroche *et al.*[23] were generally consistent with the observed neutron total and scattering cross sections. However, detailed discrepancies between measured and calculated neutron total cross sections of ^{182}W suggest smaller quadrupole or alternate deformations and/or additional channel coupling as discussed by Delaroche.[32] At low energies the contribution of CN scattering was large and not unambiguously calculable from basic concepts. At higher energies uncertainties associated with statistical level parameters[28] were a concern. Comparisons of measured and calculated cross sections for the excitation of the β- and γ-vibrational bands of ^{186}W suggested that the direct excitation of these bands makes a significant contribution to the neutron inelastic-scattering processes. Such vibrational coupling will influence the choice of general model parameters.

Some of the above physical questions might be elucidated by additional measurements. Studies of the $(n;n,'\gamma)$ process have the potential for resolving level ambiguities, particularly in ^{186}W. Precise studies of the (n,n') process as related to the excitation of β- and γ-vibrational bands, particularly in ^{186}W, could make possible rigorous investigation of vibrational couplings and their impact on the selection of general model parameters.

ACKNOWLEDGMENTS

We are generally indebted to a number of members of the Applied Nuclear Physics Section, Applied Physics Division, Argonne National Labo-

ratory for their generous assistance in this work. In addition, we are particularly indebted to Dr. J. Delaroche and Dr. P. Moldauer and to Professor A. Bodmer for their advice as to the relevant physical interaction mechanisms. This work supported by the U. S. Department of Energy.

[1]*Table of Isotopes,* 7th ed., edited by C. M. Lederer and V. S. Shirley (Wiley, New York, 1978).

[2]D. Chase, L. Wilets, and A. Edmonds, Phys. Rev. 110, 1080 (1968).

[3]D. Coope, S. Tripathi, M. Schell, J. Weil, and M. McEllistrom, Phys. Rev. C 16, 2223 (1977).

[4]R. Shamu, E. Bernstein, D. Blondin, J. Ramirez, and G. Rochau, Phys. Lett. 45B, 241 (1973).

[5]Ch. Lagrange, Proceedings of Specialist's Meeting on Fast-Neutron Scattering on Actinide Nuclei, Paris, 1982, OECD Report NEANDC-158 "U," p. 116.

[6]P. T. Guenther, thesis, University of Illinois, 1977, available from University Microfilms International.

[7]P. Guenther, D. Havel, and A. Smith, Argonne National Laboratory Report ANL/NDM-16, 1975, available from the National Technical Information Service.

[8]P. Guenther, A. Smith, and J. Whalen, Argonne National Laboratory Report ANL/NDM-56, 1981, available from the National Technical Information Service.

[9]The authors are indebted to Oak Ridge National Laboratory for the fabrication of the tungsten samples.

[10]A. Smith, P. Guenther, G. Winkler, and J. Whalen, Nucl. Phys. A332, 297 (1979).

[11]D. Miller, *Fast Neutron Physics,* edited by J. Marion and J. Fowler (Interscience, New York, 1963), Vol. II.

[12]A. Smith, R. Holt, and J. Whalen, Argonne National Laboratory Report ANL/NDM-43, 1978, available from the National Technical Information Service; see also, C. Fu and F. Perey, At. Data Nucl. Data Tables 22, 249 (1978).

[13]A. Smith, P. Guenther, and R. Sjoblum, Nucl. Instrum. Methods 140, 397 (1977).

[14]J. Hopkins and G. Breit, Nucl. Data A9, 137 (1971).

[15]W. Poenitz, J. Whalen, and A. Smith, Nucl. Sci. Eng. 78, 333 (1981).

[16]P. Guenther, W. Poenitz, and A. Smith, Proceedings of the Conference on Nuclear Data Evaluation Methods and Procedures, Brookhaven National Laboratory Report BNL-NCS-51363, 1981.

[17]J. F. Whalen, Argonne National Laboratory Report ANL-7210, 1966.

[18]R. Martin, F. Yergin, R. Augustson, N. Kaushal, H. Medicus, and E. Winhold, Bull. Am. Phys. Soc. 12, 106 (1967).

[19]D. Foster and D. Glasgow, Phys. Rev. C 3, 576 (1971).

[20]Brookhaven National Laboratory Report BNL-325, 1976.

[21]See A. Lane and R. Thomas, Rev. Mod. Phys. 30, 257 (1958).

[22]D. Lister, A. Smith, and C. Dunford, Phys. Rev. 162, 1077 (1967).

[23]J. Delaroche, G. Haouat, R. Shamu, J. Lackhar, M. Patin, J. Sigaud, and J. Chardin, Proceedings of the Conference on Nuclear Cross Sections for Technology, NBS Pub. NBS-SP-594, 1980; and Phys. Rev. C 23, 136 (1981).

[24]T. Tamura, Rev. Mod. Phys. 37, 679 (1965).

[25]JUSTSO, a coupled-channels computational code and ABAREX, a spherical optical model code, P. A. Moldauer, private communication.

[26]W. Hauser and H. Feshbach, Phys. Rev. 87, 366 (1952).

[27]P. A. Moldauer, Nucl. Phys. A344, 188 (1980); see also Phys. Rev. C 12, 744 (1975).

[28]A. Gilbert and A. Cameron, Can. J. Phys. 43, 1446 (1965).

[29]P. A. Moldauer, Proceedings of the Conference on Nuclear Data Evaluation Methods and Procedures, Brookhaven National Laboratory Report BNL-NCS-51363, 1981.

[30]B. Barrett, private communication.

[31]T. Tamura, Oak Ridge National Laboratory Report ORNL-4152, 1967, Appendix A.

[32]J. P. Delaroche, Proceedings of the International Conference on Nuclear Data for Science and Technology, Antwerp, 1982.